5th International Conference of the International Commission of Agricultural and Biosystems Engineering (CIGR)

Hosted by the Canadian Society for Bioengineering (CSBE/SCGAB)
Virtually from Québec City, Canada – May 11-14, 2021

THERMAL MODELLING OF GREENHOUSE USING 1D LUMPED CAPACITANCE MODEL

ALEX NAUTA[1], WILLIAM DAVID LUBITZ[2], SYEDA TASNIM[3], SHOHEL MAHMUD[4]

[1] University of Guelph, School of Engineering. 50 Stone Rd E, Guelph, ON, Canada. <anauta@uoguelph.ca>
[2] University of Guelph, School of Engineering. 50 Stone Rd E, Guelph, ON, Canada. <wlubitz@uoguelph.ca>
[3] University of Guelph, School of Engineering. 50 Stone Rd E, Guelph, ON, Canada. <stasnim@uoguelph.ca>
[4] University of Guelph, School of Engineering. 50 Stone Rd E Guelph, ON, Canada. <smahmud@uoguelph.ca>

CSBE21796 – Presented at CIGR 2021 General Session

ABSTRACT The energy budget and thermal conditions in a greenhouse located at the Guelph Center for Urban and Organic Farming were examined for winter conditions. Measurements of actual conditions were collected at the site for a one week period, including greenhouse air and soil temperature, outside air temperature, solar radiation, and wind speed. A one-dimensional transient lumped capacitance model was developed to predict greenhouse interior conditions based on exterior weather. The model accounted for radiation, conduction and convection heat transfer occurring within the greenhouse structure. Model elements included the glazing, the internal air and several soil layers. The model was formulated explicitly and predicts time-series results by stepping forward in time from initial conditions based on the assumed greenhouse properties and initial measured temperatures. Model accuracy was evaluated by comparing measured internal air and soil temperature to model predictions. Large variations were found in the literature for treatment of several aspects of this type of greenhouse model, including infrared emissivity of the glazing film, the radiant sky temperature model, and air leakage relationships. It was found that the model accuracy can be very sensitive to these factors. Overall, the MAE and RMSE for the simulated air temperatures versus measurements at baseline conditions were 3.46°C and 4.25°C, respectively. For the soil temperatures, the MAE and RMSE were 3.37°C and 4.28°C, respectively.

Keywords: thermal modelling; greenhouse; emissivity; lumped capacitance; IR radiation; polyethylene glazing; soil temperature; natural convection; conductive heat transfer

LITERATURE REVIEW AND BACKGROUND INFORMATION The interior microclimate within a greenhouse has a significant impact on the greenhouse crop. The ability to accurately predict the interior microclimate based on external weather and greenhouse operating conditions would allow growers to design better greenhouses and optimize growing strategies. There are several approaches to modelling the microclimate within a specific greenhouse. Detailed simulations using computational fluid dynamics (CFD) are possible and can be accurate, but are computationally intensive and require detailed knowledge of initial conditions. These CFD models typically only allow for simulating one operating condition, rather than predicting conditions dynamically over long periods of time. For this reason, many researchers focus on reduced-complexity lumped-capacitance models based on defining sets of mathematically-efficient equations that describe the heat transfer processes within the greenhouse (Roy et al., 2002). Since these models are mathematically efficient, they can be used in conjunction with time-series weather data to predict the evolution of the greenhouse microclimate over time, and to explore changes in greenhouse properties, operating protocols or weather.

Lumped Capacitance Greenhouse Models A transient, one dimensional lumped capacitance greenhouse energy model was developed for this study. In this type of model, the greenhouse is abstracted into a series of layers that are assumed to have uniform properties, such as temperature, density and heat capacity. For this project, the layers consisted of glazing, interior air, and several soil layers. The thermal pathways between the layers are defined and quantified, and typically include conduction, convection and radiation heat transfer, as appropriate. Some models also include energy transfer associated with water vapor. Heat fluxes between layers are calculated at each time step in the model, and used to find temperature changes between time steps. To calculate the transient temperature in each layer, a time step is applied and the solution is stepped forward in time explicitly. Some models in the literature use other methods to solve the governing equations rather than explicitly formulated forward stepping in time. Table 1 summaries previous greenhouse energy models that use lumped capacitance.

There is often variation in the literature on how to best model some heat transfer pathways. For example, Table 2 shows the range of convective heat transfer coefficient relationships considered in the model in this study. Equations used as baselines in this study are marked with an asterisk. In Table 2, *u* is wind speed, *T* is a layer temperature, and *h* is heat transfer coefficient, typically in units of W/m^2K.

Table 1: Summary of lumped capacitance greenhouse energy models

Type/Location	Brief Comments	Reference
Single-span, semi-cylindrical in Portugal	Developed over nighttime conditions, assumed inside ground, cladding and outside air were at freezing temperature. No convection or conduction heat transfer accounted for, only thermal radiation, and model accuracy unknown.	(Silva & Rosa, 1987)
Asymmetric overlap roof, India	Predicted air and plant temperature, compared to measured data. Validated over two 16 hour periods, used Jacobian iterative method to find temperatures at each hour.	(Sethi, 2018)
High tunnel greenhouse, Guelph, ON	Used high resolution data to predict interior air and soil temperatures. Accounted for impact of cloud cover on radiative sky temperature. Ten layers included in model.	(Ghose & Lubitz, 2018)
Unheated commercial greenhouse, Israel	Predicted air and crop temperatures, as well as RH over 51 day period for greenhouse growing tomatoes.	(Zhang, Mahrer, & Margolin, 1997)
Numerous greenhouses in Italy, Holland, Texas and Arizona	Model predicts air temperature, vapor pressure and CO_2 concentration. Validated against greenhouse data sets from various climates	(Vanthoor, Stanghellini, van Henten, & de Visser, 2011)
Three-span Azrom type greenhouse, Zimbabwe	Model ran over one year, with one minute time step. Calibration period conducted over four weeks to optimize parameters using empirical data.	(Mashonjowa E. , Ronsse, Milford, & Pieters, 2013)

Table 2: Range of equations considered for convective heat transfer coefficients

Equation	Pathway	Comments	Reference
$\boldsymbol{h = 7.2 + 3.84u}$ *	Glazing to outdoor air	Derived from experimental data, plastic glazing used	(Garzoli & Blackwell, 1981)
$\boldsymbol{h = 0.95 + 6.76u^{0.49}}$ $\boldsymbol{u \leq 6.3\ m/s}$	Glazing to outdoor air	Derived from experimental data, PE glazing	(Papadakis, Frangoudakis, & Kyritsis, 1992)
$\boldsymbol{h = 3.49u}$	Glazing to outdoor air	Derivation unknown	(Roy, Boulard, Kittas, & Wang, 2002)
$\boldsymbol{h = 2.21(T_{air} - T_{cov})^{0.33}}$ $\boldsymbol{(0.3 < T_{air} - T_{cov} < 13.8°C)}$ *	Interior air to glazing	Derived from experimental data, PE glazing	(Papadakis, Frangoudakis, & Kyritsis, 1992)
$\boldsymbol{h = 3.3(abs(T_{air} - T_{cov}))^{0.33}}$	Interior air to glazing	Derivation unknown	(Roy, Boulard, Kittas, & Wang, 2002)
$\boldsymbol{h = 4.3(T_{air} - T_{cov})^{0.25}}$	Interior air to glazing	Derived from experimental data, PVC glazing	(Kittas, 1986)
$\boldsymbol{h = 10(abs(T_{soil} - T_{air}))^{0.33}}$ *	Soil to air	Derivation unknown	(Roy, Boulard, Kittas, & Wang, 2002)
$\boldsymbol{h = 5.2(abs(T_{soil} - T_{air}))^{0.33}}$	Soil to air	Derivation unknown	(Roy, Boulard, Kittas, & Wang, 2002)
$\boldsymbol{h = 3.4(abs(T_{soil} - T_{air}))^{0.33}}$	Soil to air	Derivation unknown	(Roy, Boulard, Kittas, & Wang, 2002)

Similarly, the air leakage relationships considered in the model can be seen below in Table 3, where again *u* represents the wind speed in m/s, and *ACH* is the air exchange (greenhouse volumes per hour) due to infiltration. The Vanthoor et al (2011) relationship was used as the baseline. In the Vanthoor et al (2011) model, $c_{leakage}$ is a dimensionless constant of 0.0001, while the *ACH* must be calculated from $f_{leakage}$ using the surface area and volume of the greenhouse.

Table 3: Air leakage relationships considered in this study

Equation	Comments	Reference
$\boldsymbol{ACH = 1 + u}$	Not derived from empirical data. Units of *u*: m/s	(Ghose & Lubitz, 2018)
$\boldsymbol{f_{leakage}\ (m^3 m^{-2} s^{-1}) = 0.25 \times c_{leakage}}$ $\boldsymbol{u}$ < 0.25m/s $\boldsymbol{f_{leakage}\ (m^3 m^{-2} s^{-1}) = u \times c_{leakage}}$ $\boldsymbol{u}$ > 0.25m/s *	Derivation unknown, requires greenhouse volume and surface area to find air exchange rate	(Vanthoor, Stanghellini, van Henten, & de Visser, 2011)
$\boldsymbol{ACH = 3.4}$	Based on average from experimental results	(Mashonjowa E. , Ronsse, Milford, Lemeur, & Pieters, 2010)
$\boldsymbol{ACH = 0}$	Control, no leakage assumed	N/A

Infrared (IR) emissivity is also an important factor in greenhouse heat transfer. Values of IR emissivity used in past studies have varied widely (Table 4). A value of 0.9 was assumed as the baseline for this study.

Table 4: IR emissivity values for cover considered in this study

Value	Comment	Reference
0.2	Value used for standard PE glazing, derivation unknown	(Pieters & Deltour, 1997)
0.4	Used for PE cover in Israel, derivation unknown	(Zhang, Mahrer, & Margolin, 1997)
0.7	Used on high tunnel greenhouse in Guelph, not derived empirically	(Ghose & Lubitz, 2018)
0.9 *	Value used for double-PE greenhouses in study, not derived empirically	(Vanthoor, Stanghellini, van Henten, & de Visser, 2011)

Radiation heat transfer from the greenhouse to the sky can be modelled assuming a radiative sky temperature. The range of radiative sky temperature models used in the study can be seen summarized below in Table 5. The Berdahl & Martin (1984) equation was used as the baseline. In the equations, σ is the Stefan-Boltzmann constant, *CF* is the cloudiness factor (0-1), and e_{sky} is the emissivity of the sky (0-1).

Table 5: Radiant sky temperature equations considered

Equation	Comment	Reference
$T_{sky} = 0.0375\, T_{amb}{}^{1.5} + 0.32\, T_{amb}$	Derived using cloudiness index from 68 American cities, accuracy unknown	(Fuentes, 1987)
$T_{sky} = ((1 - CF) e_{sky}\, T_{amb}{}^{4} + CF\, (T_{amb}{}^{4} - \left(\frac{9}{\sigma}\right)))^{0.25}$	Derivation unknown	(Vanthoor, Stanghellini, van Henten, & de Visser, 2011)
$T_{sky} = CF\, T_{amb} + 0.0552\, (1 - CF)\, T_{amb}{}^{1.5}$	Used in Mediterranean context, accuracy/derivation unknown	(Wang & Boulard, 2000)
$T_{sky} = T_{amb}(e_{sky} + (1 - e_{sky}) CF)^{0.25}$	Derived using measurements from six American cities, accuracy unknown	(Berdahl & Martin, 1984)
$T_{sky} = T_{amb}$	Control scenario, where radiant sky temperature equals ambient temperature	N/A

METHODOLOGY

Experimental Data The greenhouse microclimate data used for model evaluation for this project was collected by Dr. Lubitz at the Guelph Centre for Urban Organic Farming (GCUOF) at the University of Guelph Arboretum during March 2014. The greenhouse was 14.6 m long, 9.1 m wide, and 5.5 m tall, and had traditional polyethylene glazing as the roof material (Fig. 1). The greenhouse floor was a combination of well worked soil and wood chips, and plant covers were present (Lubitz, 2015). Tree rows to the west and northwest protected the greenhouse from strong winds (Lubitz, 2015). All vents and main doors were kept closed throughout the measurement period. Measured data included air temperature (inside radiation shield) and soil temperature inside the greenhouse, and outside solar radiation (global horizontal irradiance), air temperature (in radiation shield), wind speed and direction (2 m above ground level). Data was recorded continuously for a one week period at a resolution of one minute. Lubitz (2015) provides more details. For this study, some sky temperature models required cloud cover fraction data, which was not recorded during the experiment. The average cloud covered fraction for each day from March 5th to March 10th, 2014 was obtained afterwards and incorporated into the dataset (Guelph Historical Weather, 2020). Shown in Fig. 2 is the measured indoor air, outdoor air, and soil (5 cm below surface) temperatures, as well as the solar radiation, that were collected during the duration of the experiment.

Figure 1. GCUOF Greenhouse, March 2014

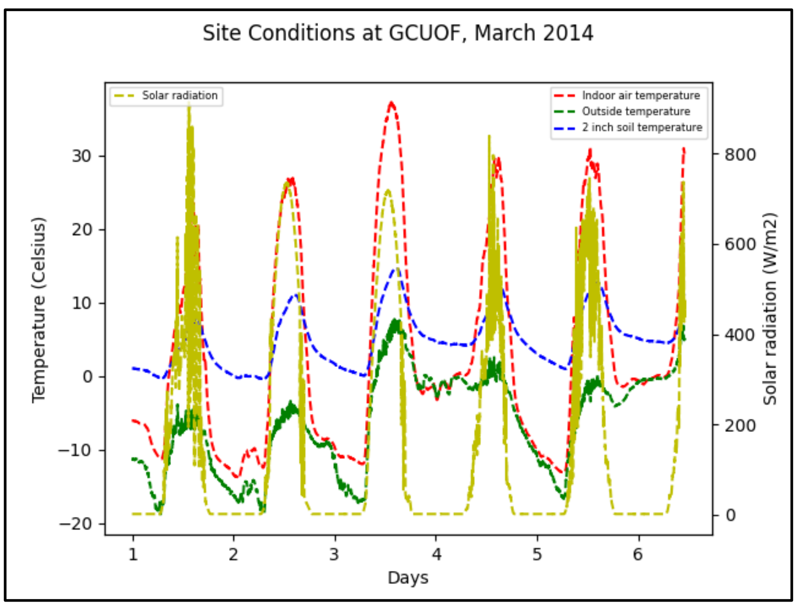

Figure 2: Measured site conditions at GCUOF, March 2014

Greenhouse Model The greenhouse was abstracted to consist of a series of adjacent regions or layers. From the top, these regions were the glazing, air space, a thin soil surface layer and several deeper soil layers, shown in Fig. 3. Conditions in each layer, such as temperature, are represented by single values of average conditions for the entire layer. All processes are assumed to be one-dimensional: it was assumed that no significant heat transfer occurred through the walls. For the soil layers, the top layer was assumed the thinnest, at 2 mm, while the bottom layer was the thickest, at 1.28 m. During the period of time when the data was collected, the greenhouse vents were kept closed and no crops were being grown (Lubitz, 2015). The recorded data had a time step of sixty seconds, however, a smaller time step of six seconds was used internally in the model to assure model stability. This means there were ten simulation steps for each data measurement.

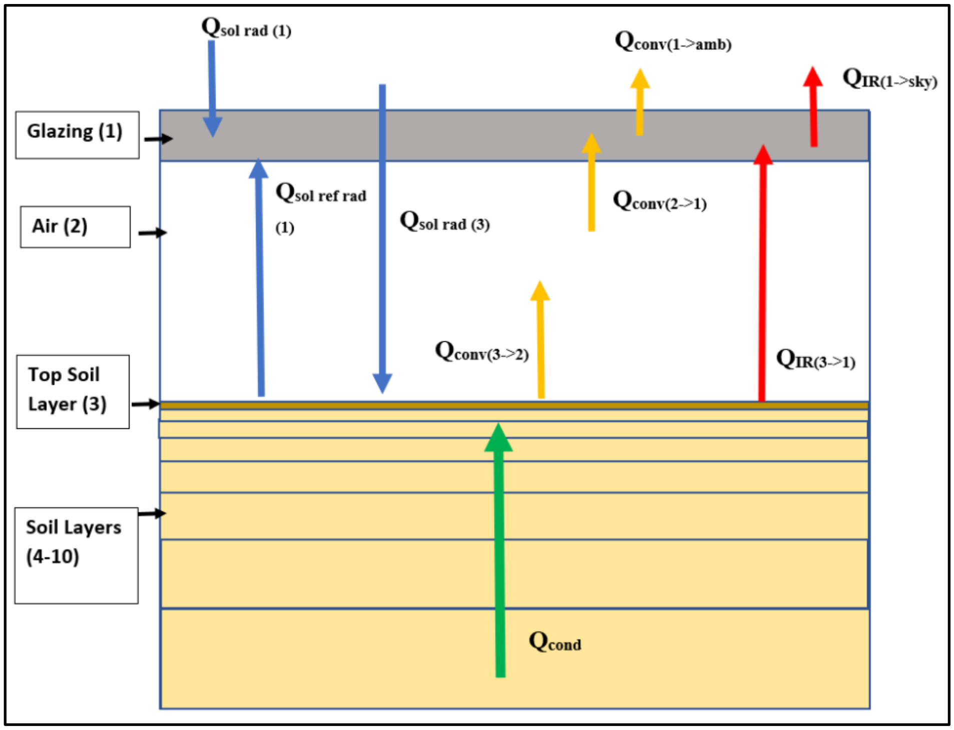

Figure 3: Schematic of greenhouse energy transfers

At each time step, the outdoor weather data, such as the ambient temperature and wind speed, were read from the measured data to be used for calculations. The model did not use any data from inside the greenhouse: this data was only used after model runs to evaluate model performance. Once the simulation of the entire week was completed, error analysis was conducted to find the RMSE and MAE of the model results for air and soil temperature versus measurements. Finally, the simulation results were plotted against the measured data to allow for a graphical analysis: an example is shown in Fig. 4.

The temperature change for each layer over a period of time equal to the time step *dt*, denoted as dT_{layer}, was solved at each time step using a combination of measured experimental data, assumed material parameters, and simulated values. A summary of this energy balance equation for each layer is shown below, with heat transfer flux from solar radiation, IR radiation, convection and conduction considered. The glazing layer is denoted as layer 1, the air layer is 2, the top soil layer is 3, and the bottom soil layers are denoted as 4-10 (Fig. 3).

$$dT_1 = \frac{dt\ (Q_{sol\,rad_1} + Q_{sol\,rad_{ref_1}} + Q_{conv\,2\to1} + \ Q_{IR\,3\to1} - Q_{conv\,1\to amb} - Q_{IR\,1\to sky})}{c_1\ \rho_1\ dx_1} \qquad (1)$$

$$dT_2 = \frac{dt\ (Q_{conv\,3\to2} - Q_{conv\,2\to1})}{c_2\ \rho_2\ dx_2} \quad (2)$$

$$dT_3 = \frac{dt\ (Q_{sol\,rad_3} + Q_{cond\,4\to3} - Q_{conv\,3\to2} - Q_{IR\,3\to1})}{c_3\ \rho_3\ dx_3} \quad (3)$$

$$dT_i = \frac{dt\ (Q_{cond\,i+1\to i} - Q_{cond\,i\to i-1})}{c_i\ i\ dx_i} \quad (4)$$

*Note that Equation 4 is used for layers *i* = 4 through 9, with only the layer subscripts changing

$$dT_{10} = \frac{dt\ (-Q_{cond\,10\to9})}{c_{10}\ \rho_{10}\ dx_{10}} \quad (5)$$

In the equations above, *Q* is the rate of heat transfer (in W/m^2), with numeric subscripts denoting layer number, and "amb" representing outside ambient conditions. Heat transfer mechanisms are denoted as conduction ("cond"), convection ("conv"), solar radiation ("sol rad") or infrared radiation ("IR"). Absorptivity and transmissivity of layer *i* are α_i and τ_i respectively, with additional subscripts representing solar ("sol") or infrared ("IR") radiation. The model time step is *dt*, while ρ_I and c_i are the density and heat capacity of the material comprising layer *i*. Infrared emissivity of layer *i* is ε_i while sky emissivity is ε_{sky}. Shown below in Table 6 are the heat transfer equations used in the model, where *G* represents the measured solar irradiance, in W/m^2. Table 7 further defines and gives values used for these variables. The model was implemented in the open-source programming language Python.

Table 6: Description of heat transfer equations

Description of Heat Transfer Equation	Equation
Solar irradiance absorbed by glazing	$Q_{sol\,rad\,1} = G\ \alpha_1$
Transmitted solar irradiance absorbed by soil	$Q_{sol\,rad\,3} = G\ \tau_{sol_1}\ (1 - \alpha_3)$
Solar radiation reflected from soil, absorbed by glazing	$Q_{sol\,rad_{ref_1}} = G\ \tau_{sol_1}\ \alpha_3\ \alpha_1$
Convection from soil to inside air	$Q_{conv\,3\to2} = h_{3\to2}(T_3 - T_2)$
Convection from inside air to glazing	$Q_{conv\,2\to1} = h_{2\to1}(T_2 - T_1)$
Convection from glazing to outdoor air	$Q_{conv\,1\to amb} = h_{1\to amb}(T_1 - T_{amb})$
Infra-red radiation from glazing to sky	$Q_{IR\,1\to sky} = \sigma(\epsilon_1(T_1)^4 - \varepsilon_{sky}(T_{rs})^4)$
Infra-red radiation from ground absorbed by glazing	$Q_{IR\,3\to1} = \sigma(1 - \tau_{IR,1})(\epsilon_3(T_3)^4 - \varepsilon_1(T_1)^4)$
Conductive heat transfer for each soil layer *(i* is layer number)	$Q_{cond} = \frac{k_3(T_i - T_{i-1})}{0.5dx_i + 0.5dx_{i-1}}$

A single variable sensitivity analysis was performed at baseline conditions for the air leakage relationship, the radiant sky temperature model, and the glazing IR emissivity. Furthermore, ten randomized input arrays were tested, with each of the three parameters under consideration subjected to a single variable sensitivity analysis at each scenario.

RESULTS AND DISCUSSION For the 1D lumped capacitance model, a baseline scenario was defined for the system parameters, which is summarized in Table 7. These baseline parameters were selected based on literature values and results, with several coming from the work of Ghose & Lubitz (2018).

Table 7: Summary of baseline parameters used for Python model

Parameter	Value	Variable	Parameter	Value	Variable
IR trans of glazing	0.45	$\tau_{IR,1}$	Soil conductivity (W/m*K)	0.15	k_{3-10}
Glazing solar radiation reflectivity	0.2	α_1	Soil heat capacity (J/kg*K)	1850	c_{3-10}
Glazing solar radiation transmissivity	0.6	$\tau_{sol,1}$	Soil IR emissivity	1.0	$\varepsilon_{IR,3}$
Glazing heat capacity (J/kg*K)	2000	c_1	Sky IR emissivity	0.74	ε_{sky}
Glazing density (kg/m^3)	905	ρ_1	Air heat capacity (J/kg*K)	1007	c_2
Glazing thermal conductivity (W/m*K)	0.45	k_1	Air density (kg/m^3)	1.16	ρ_2
Soil reflectivity	0.2	α_3	Thermal conductivity of air (W/m*K)	0.026	k_2
Soil density (kg/m^3)	2050	ρ_{3-10}			

The simulation was run using the values in Table 7 and recorded weather data at the site. Fig. 4 shows the simulation results for air temperature and soil temperature compared with the corresponding measured data. The simulated temperatures generally match the overall trends of the data for both, but appear to match the air temperature better due to the larger temperature range observed for air versus soil. Note the differences in vertical scale range in the two plots in Fig. 4.

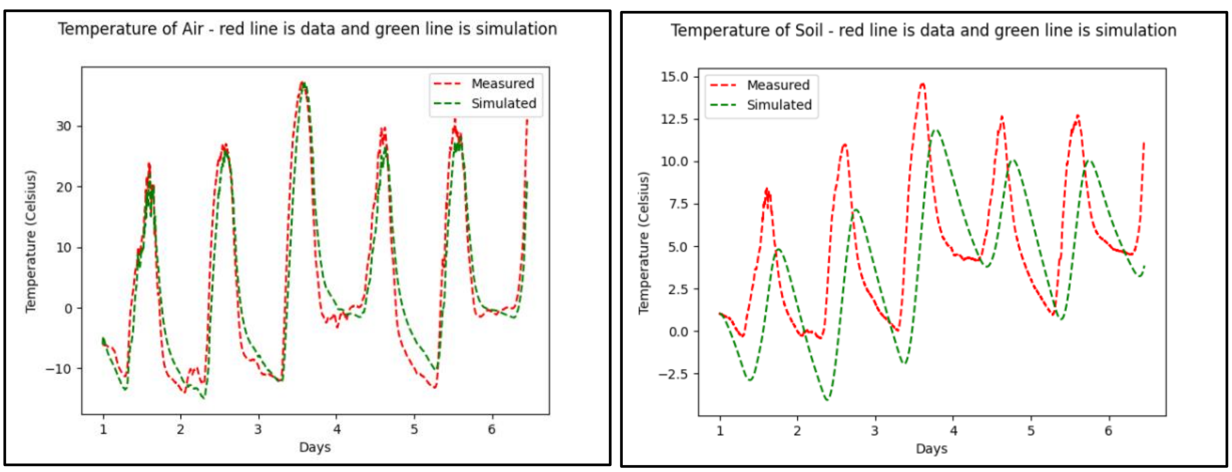

Figure 4. Air and soil temperatures - simulation versus measurements for baseline conditions

A RMSE of 4.28°C for the simulated soil temperature (model layer 5) was found, while the RMSE was 4.25°C for the air temperature. The MAE was 3.37°C and 3.46°C for the simulated soil and air temperatures, respectively.

Sensitivity Analysis Using the baseline conditions, a single variable sensitivity analysis was conducted on three variables of interest, which were the IR glazing emissivity ($\varepsilon_{IR,1}$), the leakage relationship (*ACH*), and the radiant sky temperature (T_{RS}) model. These can be seen below in Figure 5-6, with the RMSE and MAE for soil and air temperatures shown for each.

Fig. 5 shows that IR emissivity values of 0.9 and 0.7 produced lower errors, while 0.2 and 0.4 resulted in higher errors. In the case of air leakage, it can be seen that the lowest errors were from the control case and from Vanthoor et al. (2011). This would seem to signify that there was little to no air leakage occurring at the greenhouse over the duration of data collection, which is backed up by the relatively low wind speeds observed at the site, which averaged less than 0.5m/s. For the radiant sky temperature models in Fig. 6, there do not appear to be one or two models that were consistently better than the rest, making further analysis necessary.

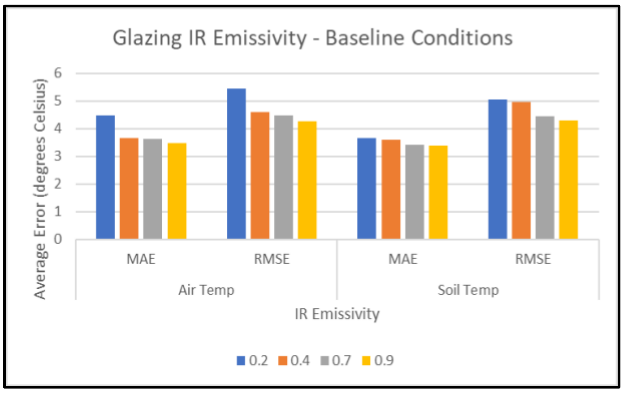

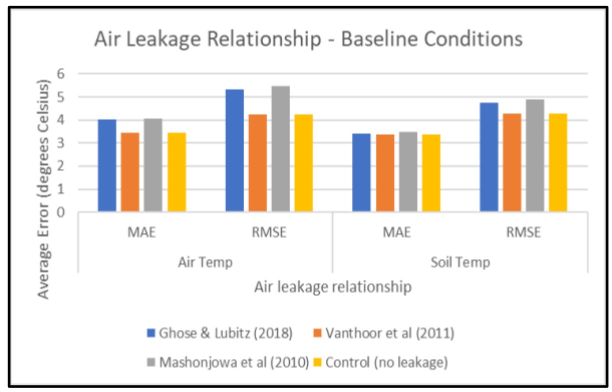

Figure 5: Single variable sensitivity analysis for IR glazing emissivity and air leakage at baseline conditions

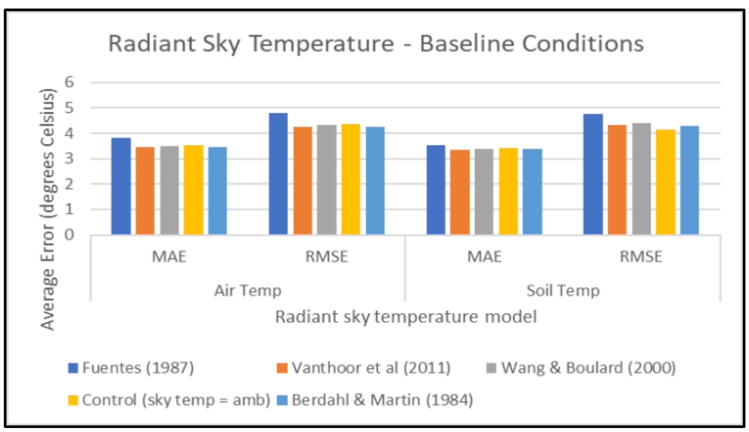

Figure 6: Single variable sensitivity analysis for radiant sky temperature models at baseline condition

To expand on the accuracy of the sensitivity analysis for the three parameters under consideration, ten randomized input configurations were tested for the model. At each configuration, the three parameters were subject to a single variable sensitivity analysis. The variables that were modified in the model for the input configurations besides the three of focus included the three separate convective coefficient equations mentioned earlier in the report, the soil IR emissivity, the soil heat capacity, the soil thermal conductivity, and the glazing transmissivity and reflectivity to solar radiation.

The optimal assumed IR emissivity of the glazing was found to be 0.7 and 0.9, with 0.2 and 0.4 resulting in larger overall errors for each testing scenario. This is useful information for future model development, as literature results showed a wide range of values used for polyethylene greenhouse covers. Also, the two configurations with the lowest prediction accuracy both had an IR emissivity of 0.2 for the glazing. To illustrate how important just one value is on the overall model accuracy, the single variable sensitivity analysis for the IR glazing for one configuration had a MAE of 21.6°C for the air temperature at an emissivity value of 0.2. When 0.7 was used instead, the MAE was 4.04°C for the air temperature. For this same example, the MAE of the soil temperature decreased from 10.2°C to 3.92°C. Direct measurement of IR emissivity of common greenhouse glazing materials would be the ideal solution to reduce uncertainty with this variable.

Results were mixed for the air leakage models. The Mashonjowa et al. (2011) relationship was used in the most simulations with lowest overall error, while the control case (assuming no air leakage) produced the lowest errors on two occasions. This may be a result of the Mashonjowa et al. (2011) air leakage value being derived from experimental measurements at a polyethylene greenhouse in Zimbabwe. While the Vanthoor et al. (2011) and the Ghose & Lubitz (2018) models did not produce the lowest error in any of the ten randomized configurations tested, they still yielded overall results in the same relative error range. Evidently, more work will need to be done to define the optimal air leakage relationship for this greenhouse, which will likely require additional experimental data sets for validation. Improved methods to estimate or quantify air leakage relationships in specific greenhouse would be useful.

Similarly, the radiant sky temperature model comparisons had mixed results. The Fuentes (1987) relationship achieving the lowest errors in seven of the ten configurations. The Wang & Boulard (2000) and Vanthoor et al. (2011) models did not have any instances where they produced the lowest errors, but should not be discarded as their error values were often close in magnitude.

These findings suggest that further testing is needed to find the optimal radiant sky temperature model, as well as the air leakage relationship. A multivariable sensitivity analysis could be conducted, where every possible configuration is simulated, which would allow for consistently strong performers to be identified more readily. Higher emphasis could also be placed on examining model configurations that produce low overall errors, such as the baseline scenario in this study.

Discussion Limitations of the model presented in this study include not accounting for moisture in the energy balance. While the impact of energy exchange through moisture processes is likely low in the case examined here (closed greenhouse in winter with no irrigation or significant plant transpiration), energy exchange through these mechanisms will be significant in most other cases of interest (warmer temperatures, active crops).

Potential applications for the greenhouse model described here include being able to predict greenhouse energy requirements based on outdoor weather conditions and site-specific properties. This would help growers determine what air and soil temperatures would be expected at a specific time. If the model was expanded to include additional lumped layers for plants, and multiple air layers if a thermal curtain is present, then it could be expanded to commercial greenhouses. Any supplemental heating, such as from hot water piping, would be accounted for, which would help growers predict their energy costs over a growing season. Potential energy saving applications, such as phase change materials or earth air heat exchangers, could be evaluated to assess their impact and whether they were worth implementing. The authors plan to continue model development.

Overall, the model compares well to models in the literature (Table 1). Table 8 shows a summary of the air temperature RMSE and MAE for these models, with the results from this project also included. Worth noting is that the literature models with low errors are from climate zones much different than Guelph, and likely experience lower daily temperature fluctuations. Models with hourly, rather than minute, resolution also typically have lower mean error levels due to the averaging of short time scale effects.

Table 8: RMSE and MAE for air temperature results from literature

Model	**RMSE (°C)**	**MAE (°C)**
(Sethi, 2018)	3.7	N/A
(Ghose & Lubitz, 2018)	1.7-7.8	1.4-5.2
(Zhang, Mahrer, & Margolin, 1997)	1.2	N/A
(Vanthoor, Stanghellini, van Henten, & de Visser, 2011)	3.3-8.0	N/A
(Mashonjowa E. , Ronsse, Milford, & Pieters, 2013)	N/A	1.3-1.8
Current study	4.25	3.46

CONCLUSION A lumped capacitance greenhouse energy model was developed and applied to a small, closed passive greenhouse in winter. Using the baseline conditions for the 1D lumped capacitance model implemented in Python resulted in MAE and RMSE of 3.46°C and 4.25°C for the simulated air temperature in comparison to the measured air temperature over the six day experiment. The MAE and RMSE for the soil temperature analysis at baseline conditions was 3.37°C and 4.28°C. Using a single variable sensitivity analysis at ten randomized input configurations, the optimal IR emissivity for the polyethylene glazing was determined to be 0.7 and 0.9. The optimal radiant sky temperature and air leakage models for the greenhouse were not able to be directly concluded in this report due to mixed results, but they will continue to be examined as the research project progresses.

This project provides a foundation to build on for conducting energy simulations of larger, more complex commercial greenhouses, where the potential applications for the model are higher. Growers could potentially use the model to aid in decision making for temperature scheduling, crop planting and harvesting, as well as the estimated impact of installing energy saving technology such as phase change materials. The authors are continuing to model development and testing for these applications.

ACKNOWLEDGEMENTS This study was completed as part of a larger project investigating the energy use, and potential for energy savings, in commercial horticultural greenhouses funded by the Ontario Ministry of Agriculture, Food and Rural Affairs (OMFRA) Alliance – Tier I program (grant UG-T1-2020-100103 “Heat Storage to Save Energy in Ontario Greenhouses”).

REFERENCES

Berdahl, P., & Martin, M. (1984). Emissivity of clear skies. *Solar Energy, 32*(5), 663-664.

Fuentes, M. (1987). A Simplified Thermal Model for Flat-Plate Photovoltaic Arrays. *Sandia Report*(RS-8232-2I).

Garzoli, K., & Blackwell, J. (1981). An Analysis of the Nocturnal Heat Loss from a Single Skin Plastic Greenhouse. *Journal of Agricultural Engineering Research, 26*(3), 203-214.

Ghose, S., & Lubitz, W. (2018). *Thermal Modelling of Passive Solar High Tunnels Located at the Guelph Centre for Urban Organic Farming.* Guelph: University of Guelph.

Guelph Historical Weather. (2020, October). Retrieved from World Weather Online: https://www.worldweatheronline.com/guelph-weather-history/ontario/ca.aspx

Kittas, C. (1986). Greenhouse cover conductances. *Agricultural Research Center of Peloponnisos and Ipiros, 36*(3), 213-225.

Lubitz, W. (2015). *Reducing Canadian Greenhouse energy costs using highly insulating glazing* (Chapter in: Renewable Energy in the Service of Mankind I). Cham: Springer International Publishing.

Mashonjowa, E., Ronsse, F., Milford, J., & Pieters, J. (2013). Modelling the thermal performance of a naturally ventilated greenhouse in Zimbabwe using a dynamic greenhouse climate model. *Solar Energy, 91*, 381-393.

Mashonjowa, E., Ronsse, F., Milford, J., Lemeur, R., & Pieters, J. (2010). Measurement and simulation of the ventilation rates in a naturally ventilated azrom-type greenhouse in Zimbabwe. *American Society of Agricultural and Biological Engineers, 26*(3), 475-488.

Papadakis, G., Frangoudakis, A., & Kyritsis, S. (1992). Mixed, Forced and Free Convection Heat Transfer at the Greenhouse Cover. *Journal or Agricultural Engineering Research, 51*(3), 191-205.

Pieters, J., & Deltour, J. (1997). Performances of greenhouses with the presence of condensation on cladding. *Journal of Agricultural Engineering Research, 68*(2), 125-137.

Roy, J., Boulard, T., Kittas, C., & Wang, S. (2002). Convective and Ventilation Transfers in Greenhouses, Part 1: the Greenhouse considered as a Perfectly Stirred Tank. *Biosystems Engineering, 83*(1), 1-20.

Sethi, V. (2018). Thermal modelling of asymmetric overlap roof greenhouse with experimental validation. *International Journal of Sustainable Energy, 38*(1), 24-36.

Silva, A., & Rosa, R. (1987). Radiative Heat Loss inside a Greenhouse. *Journal of Agricultural Engineering Research, 37*(2), 155-162.

Vanthoor, B., Stanghellini, C., van Henten, E., & de Visser, P. (2011). A methodology for model-based greenhouse design: Part 1, a greenhouse climate model for a broad range of designs and climates. *Biosystems Engineering, 110*(4), 363-377.

Wang, S., & Boulard, T. (2000). Predicting the microclimate in a naturally ventilated plastic house in a Mediterranean climate. *Journal of Agricultural Engineering Research, 75*(1), 27-38.

Zhang, Y., Mahrer, Y., & Margolin, M. (1997). Predicting the microclimate inside a greenhouse: an application of a one-dimensional numerical model in an unheated greenhouse. *Agricultural and Forest Meteorology, 86*(3), 291-297.